Simple model for the prediction of seizure durations

Tyler Salners and Karin A. Dahmen

Department of Physics, University of Illinois at Urbana Champaign, Urbana, Illinois 61801, USA

John Beggs

Department of Physics, Indiana University, Bloomington, Indiana 47405, USA

A simple model is used to simulate seizures in a population of spiking excitatory neurons experiencing a uniform effect from inhibitory neurons. A key feature is introduced into the model, i.e., a mechanism that weakens the firing thresholds. This weakening mechanism adds memory to the dynamics. We find a seizure-prone state in a "mode-switching" phase. In this phase, the system can suddenly switch from a "healthy" state with small scale-free avalanches to a "seizure" state with almost periodic large avalanches ("seizures"). Simulations of the model predict statistics for the average time spent in the seizure state (the seizure "duration") that agree with experiments and theoretical examples of similar behavior in neuronal systems. Our study points to. different connections between seizures and fracture and also offers an alternative view on the type of critical point controlling neuronal avalanches.

I. INTRODUCTION

In the past few decades, simple models from statistical physics have proven useful for the identification and interpretation of interesting patterns of spiking neurons. In particular, efforts in the last couple of decades uncovered "neuronal avalanches" [1], which are cascades of causally connected spikes in a network of neurons. Tools from statistical physics help identify and interpret the statistics of these avalanches [1–4].

In this work, we will describe neuronal avalanches and their relation to seizures using a variation of a model initially introduced to study large earthquakes. Our results not only provide testable predictions for future experiments and evidence for a different candidate critical point controlling neurodynamics, but also uncover a potential connection between seizures and fracture.

A spike describes the rapid release of membrane potential from a neuron that has reached its spiking threshold. After spiking, the neuron releases membrane potential which is subsequently transferred through synaptic connections to other neurons in the network. Spiking neurons can trigger other neurons to spike also, leading to cascades of spiking activity (neuronal avalanches) [1–5]. Tools from statistical physics, such as the theory of phase transitions and criticality, provide simple predictions for the statistical properties of these avalanches that can be validated by experiments [1–4].

Criticality refers to features of a system smoothly crossing between two unique states via a "continuous phase transition." Spiking neuronal systems have been hypothesized to be operating near a continuous phase transition between the "absorbing" state, where the avalanches are small, and the "active" state, where avalanches proliferate through the entire system (i.e., grow macroscopically large) [6–11]. The critical

point defines the parameter values where this phase transition occurs. Near this transition, not only does the network have computational advantages [12,13], but we expect avalanches of all sizes—"power-law" distributions—which provide a testable prediction of the theory (for example, power-law exponents and scaling functions).

Specifically, the total number of spikes emitted during an avalanche (or avalanche "size"), S, can be recorded for many avalanches in an experiment to obtain a histogram, or the probability distribution of S, called $P(S)$. The statistical models predict that near criticality, this distribution will look like a power law over a broad range of sizes. The regime of avalanche sizes where the distribution can be described by such simple scaling laws is referred to as the scaling regime. Indeed, empirically observed distributions of avalanche sizes and durations resemble power laws, with the power law extending up to three or more decades in size (S) [1,3–5,12].

"Universality," a powerful feature of criticality, tells us that these scaling predictions are equivalent for entire classes of models that describe distinct microscopic details. This is likely the reason why many biologically motivated models predict the same universal scaling of the avalanche statistics [4,6–8,14–18]. These models are said to be in the same "universality class." Since earthquake models and neuron models belong to the same universality class, we expect that there are many connections between neurons and other systems such as magnets, earthquakes, nanocrystals, etc. [4]. The renormalization group (RG) identifies which properties are relevant for the scaling behavior on large scales and which ones are irrelevant. It also predicts which biologically motivated amendments of existing models alter the universality class [13,19,20]. We will use these tools to inform our model.

Here we model an excitatory population of neurons that feel an average effect of inhibitory neurons. Inhibitory

neurons send negative ionic currents when they spike, preventing more excitatory neurons from spiking soon after [21]. At the simplest level, the effect of an inhibitory neuron spike amounts to a reduction in the potential of the excitatory network.

More importantly, to include memory in an avalanche, we also introduce a mechanism that once a neuron has spiked, dynamically reduces the spiking threshold for the remainder of the avalanche. This threshold reduction (or "weakening") changes the avalanche statistics [22,23], and so is a relevant parameter (in the sense outlined in the previous paragraph). Specifically, with weakening, periodically occurring system-spanning (or "runaway") avalanches occur, which are composed of a significant amount of recurrent spiking, a feature that was recently validated by *in vitro* cortical spiking data in large avalanches [24]. These results point towards a memory mechanism such as temporary weakening of the thresholds (or temporary strengthening of the couplings to the same neuron) that affects the distribution of the spiking avalanches. In this work, we hope to draw a comparison between spiking neuronal systems and weakened elastic interfaces and survey the implications of such a connection on, e.g., seizure dynamics.

We survey the implications of this model for our understanding of the epileptic state and neuronal dynamics in general. First, we find that with the introduction of weakening, we uncover a different connection between the fracture literature and seizures [25]. This connection allows us to translate predictions for large material fracture and earthquakes into predictions for seizure time statistics. Since these predictions require no definition of an avalanche, they circumvent all ongoing controversies about the precise definition of neuronal avalanches [26]. This study also provides a different approach to the effective mechanism of seizures.

Along with the testable predictions about seizure statistics and time series properties, this work provides information about the type of critical point that underlies neuronal dynamics. Here, instead of the more common directed percolation universality class [6–11], our model suggests that the depinning class with weakening may be better suited for describing neurodynamics, at least as they are related to seizures. Lastly, an important consequence of our model is that neuronal networks require tuning to operate at the critical point, and thus their dynamics are not "self-organized critical." This observation stands in contrast to many other mechanisms in the literature that suggest self-organized criticality [1,5,7,14,16,19,27–29].

II. MODEL

To study the dynamics of a system of N spiking neurons, it is typical to define the state of the network as $\vec{V} = V_i$ where V_i is the potential of neuron i. Next, we define a neuron-dependent reset potential $V_{r,i}$, drawn from a parabolic distribution (with width w) to capture the inherent disorder of neuronal systems. We point out that here, the neuronal potential V_i is in exact analogy to the local stress τ_i from the model described in [22]. To evolve the network state in the simulation, the potential of all neurons is artificially increased until the first neuron reaches its threshold

potential, $V_{i,\text{thresh}} \equiv 1$, whence it emits a spike, reducing its own potential by $\Delta V_i = V_{i,\text{thresh}} - V_{r,i}$. The released potential is dispersed evenly to the rest of the system via the synaptic connections, increasing the potential of all other neurons by $\Delta V_{i,\text{system}} = \Delta V_i/N$. To include realistic neuronal effects, here we will introduce two features: (1) A separate population of inhibitory spiking neurons whose effect will be to suck potential out of the system with strength α. This amounts to a change in $\Delta V_{i,\text{system}} \rightarrow (1 - \alpha)\Delta V_{i,\text{system}}$. This assumption is justified by experiments that show that the number of inhibitory neurons that spike in each avalanche is proportional to the number of excitatory neurons that spike in the same avalanche (see Appendix B). (2) A threshold reduction mechanism, which has been shown to replicate experimentally resolved recurrent spiking in large neuronal avalanches [24]. After a neuron spikes, the threshold necessary for a subsequent spike is lowered, $V_{\text{thresh}} \rightarrow V_{\text{thresh}} - \epsilon \Delta V_{r,i}$, for the remainder of the avalanche, where $\epsilon \in [0, 1]$ is the strength of the weakening. The features described above can be captured by the following equation for neuron potential at time t:

$$V_{i,t} = V_{i,t-1} + \sum_{j \in \text{spiked}} \Delta V_j/N - \delta_{i,t-1}\Delta V_i, \tag{1}$$

where the sum is over all j neurons that spiked at time $t - 1$ and $\delta_{i,t-1} = 1$ if the neuron i spiked at time $t - 1$, and $\delta_{i,t-1} = 0$ otherwise.

One can show that the weakening effect is equivalent to fixing the threshold and instead increasing the gain function (or strengthening the couplings) of a neuron after it has spiked; either way, the neuron reaches the threshold faster. Though the latter may be more biologically motivated, we use the former for ease of comparison with previous work [22,25]. In the following, we will therefore discuss the behavior of our system as a function of inhibition and weakening (i.e., in $\{\alpha, \epsilon\}$ space). A graphical representation of the model described above is shown in Fig. 1.

III. RESULTS

The model described above produces dynamics in the form of avalanches. There are two predicted steady states, determined by the position of the system in $\{\alpha, \epsilon\}$ space (for the interested reader, a derivation of the following phase boundary can be found in [22], where the conservation parameter $c \equiv 1 - \alpha$ is used, in contrast to the inhibition parameter α introduced in this work). For $\alpha > \alpha^* \equiv \epsilon/(1 + \epsilon)$, in the region of Fig. 2(a) labeled "stable," the system response consists only of scale-invariant avalanches [Fig. 2(b), $\epsilon = 0$] producing a power-law distribution for the avalanche size with slope $-3/2$ [25] up to a maximum size that broadens with increasing α as $S_{\text{max}}^n \sim 2\alpha^{-2} + \mathcal{O}(\alpha^2)$ [22]. We will refer to this as the normal state. For $\alpha < \alpha^*$, in the region labeled "bistable," a second steady state is possible, consisting of temporally quasiperiodic system-spanning avalanches, with smaller scale-free avalanches in the times between them. We refer to these smaller avalanches happening in between the system-spanning avalanches as the "background activity." The size distribution thus has a power law for small sizes (from the background activity) with slope -2 [25], up to a cutoff $S_{\text{max}}^s = 2(1 - \epsilon)^2/(\epsilon - \alpha)^2 + \mathcal{O}[(\epsilon - \alpha)^2] < S_{\text{max}}^n$ [22], followed by
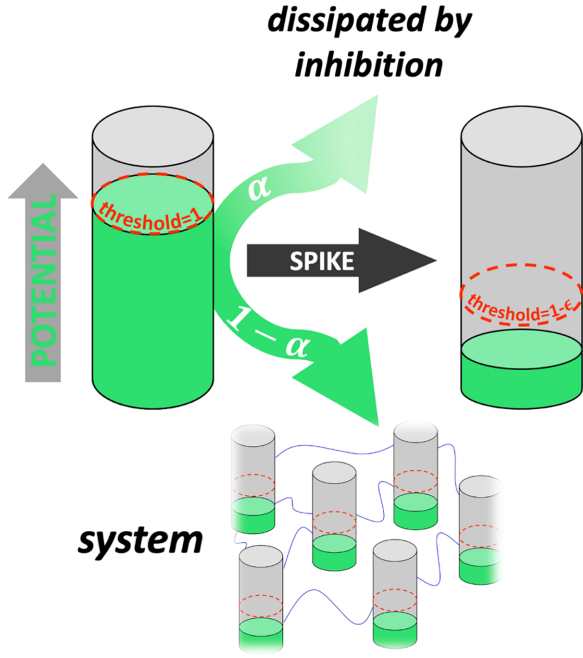
FIG. 1. Graphic of main changes to typical neuron models. Left: When a neuron reaches the threshold, it spikes, sending a portion of the potential released back into the system. The rest of the potential is dissipated by inhibition. Right: The threshold is reduced after spiking until the avalanche is complete.

the system-spanning avalanches, together yielding a bimodal distribution [Fig. 2(b), $\epsilon = 0.4$, red]. These large avalanches are referred to as runaway events and we refer to this state as the seizure state. Note how, by simply increasing inhibition, the system-spanning avalanches can be suppressed [Fig. 2(b), $\epsilon = 0.4$, green] with the power-law slope returning to $-3/2$. For ease of comparison with experiments and simulations, we show in Fig. 2(b) the complement of the cumulative distribution function (CCDF) which accordingly follows a power law of $-1/2$ and -1, in the stable and bistable regions, respectively. Constructing the CCDF from experimental and simulation data does not require the definition of bins, and therefore is preferable to the probability distribution function (PDF) option.

Since the switching times grow with the system size, for $N \to \infty$, the initial conditions (within the bistable region) determine whether the system operates in the normal or seizure steady state. For finite N, however, the probability of spontaneously switching between the two states is nonzero, and switching from one to the other is expected. This switching from the normal state into the seizure state is facilitated by a nucleation mechanism, where an avalanche of size larger than the nucleation size, $S_{cr} \sim (1-\epsilon)N/(1-\alpha)$, grows into a system-spanning avalanche [22]. The nucleation size for the seizures reflects the competition between the effect of the inhibitory neurons (plus disorder effects) and the threshold weakening effect (or, equivalently, the strengthening of the coupling). The inhibitory neurons are the brakes of the brain and their negative coupling to the excitatory neurons breaks up large avalanches into smaller ones. In contrast, the threshold weakening (or the strengthening of coupling between

neurons) tends to synchronize the firing of neurons, leading to large avalanches. For a given strength of the inhibitory neurons, at sufficiently large weakening, a given avalanche size becomes the nucleation size, i.e., the size that is able to continue growing into a large runaway avalanche. This nucleation size has been derived in a different context in [22]. The system can also transition back into the normal state from the seizure state if there are not enough neurons available to participate in a runaway event (see [22]).

This switching is visible in a typical time trace of avalanche sizes from model simulations [shown in Fig. 2(c)]. We will focus on the mode-switching process from seizure to normal state (describing the duration of the seizure state) which has a persistence time ΔT, depending on α, ϵ, N and the characteristic time needed to load a neuron to threshold, T_0. The average persistence time is predicted by our model to have the approximate form [22]

$$\langle \Delta T \rangle \approx T_0 \frac{N^{3/2}}{S_{\max}^{s}{}^2} e^{(\gamma + \gamma^2)N/S_{\max}^{s}}, \tag{2}$$

where $\gamma \equiv (\alpha^* - \alpha)/[(1-\alpha^*)(1-\alpha)]$ [22].

For a portion of $\{\alpha, \epsilon\}$ space in the unstable region [blue box, Fig. 2(a)], we extracted the first moment of time spent in the seizure state $\langle \Delta T \rangle$ from model simulations. In Fig. 3(a), we plot $\langle \Delta T \rangle$ vs weakening, for varying values of inhibition. We see that inhibition reduces the average time spent in the seizure state (i.e., $\langle \Delta T \rangle$ decreases with increasing inhibition). We also see that this reduction competes with the weakening which acts to increase $\langle \Delta T \rangle$ [see Fig. 3(a)].

As an initial comparison of the model with data, we have examined spiking signals from many hundreds of neurons in a slice culture of mouse cortex [30]. A feature of most *in vitro* spiking neuron systems is the presence of slow oscillations between a state of low activity and one of high activity, a phenomenon usually referred to as bursting [5]. We extracted times spent in each of the states (see the Appendices) and constructed complementary distribution functions to compare with the model's switching times [e.g., by identifying the high activity state with the seizure state and the low activity state with the normal state; Fig. 3(b)]. This distribution was predicted in [22] to follow Poissonian statistics, as seen in the simulation results of Fig. 3(b).

IV. DISCUSSION

Work in the past has used the idea of criticality for understanding seizures, in some cases suggesting seizures are analogous to the supercritical state [31–33]. Several experiments [34–37] have also suggested that long-range temporal correlations (LRTCs) increase before a seizure happens, due in part to "critical slowing down." This refers to the timescale of relaxation in the system becoming very large, potentially providing a powerful method to predict when seizures might happen (e.g., by measuring the Hurst exponent). Besides these preemptive features of seizures, the degree of criticality also has been shown to vary during seizures, corresponding to shallow (supercritical) power laws [31,33,34,38,39] and reduced avalanche fractal dimension [34]. The link between criticality and seizures, due to its powerful yet simple nature, has even leaked into the clinical realm [40].
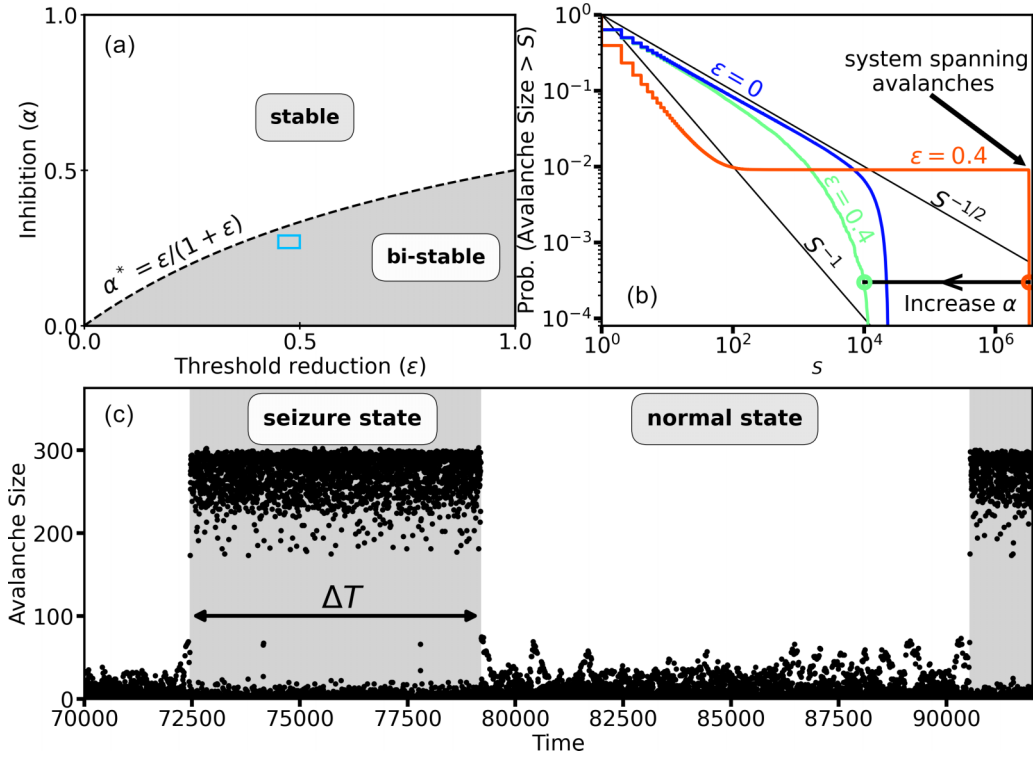
FIG. 2. Bistability between normal and seizure states in simulations. (a) Phase diagram for $\alpha, \epsilon \in [0, 1]$. Phase boundary α^* (black dashed line) separates the stable and bistable regimes. A teal perimeter highlights the region of phase space sampled for switching statistics. (b) Avalanche size distribution for weakened ($\epsilon > 0$) and nonweakened ($\epsilon = 0$) simulations. Black lines show the two critical exponents predicted in [25]. System-spanning avalanches are evident by the sharp vertical lines in the weakened case. Simulation parameters are $N = 25\,000$, $w = 0.1$, $\alpha = 0.005$ (green line: $\alpha = 0.008$). (c) Time trace of avalanche sizes in model simulations. Seizure states are highlighted in gray and ΔT marks the seizure duration. Simulation parameters are $N = 100$, $w = 2/19$, $\epsilon = 0.46$, $\alpha = 0.25$.

In this work, we predict how long seizures might last, as a function of just two simple parameters: inhibition and dynamic threshold reduction. Importantly, our work incorporates the simple dynamic threshold reduction, and so brings light to a potential memory mechanism that warrants further experimental investigation.

To understand seizures, which can be thought of as temporary episodes of bursting behavior, we focused on the

bistable phase. There, we saw that the system switches between the normal state and the seizure state. In the seizure state, the avalanche size distribution follows a power law with a bump in the tail (sometimes referred to as a "characteristic-earthquake distribution;" see [22]) reflecting the runaway avalanches [9,27]. In the normal state, there are no runaway events and the avalanches are just distributed according to a power law with a smaller cutoff. Previous work on
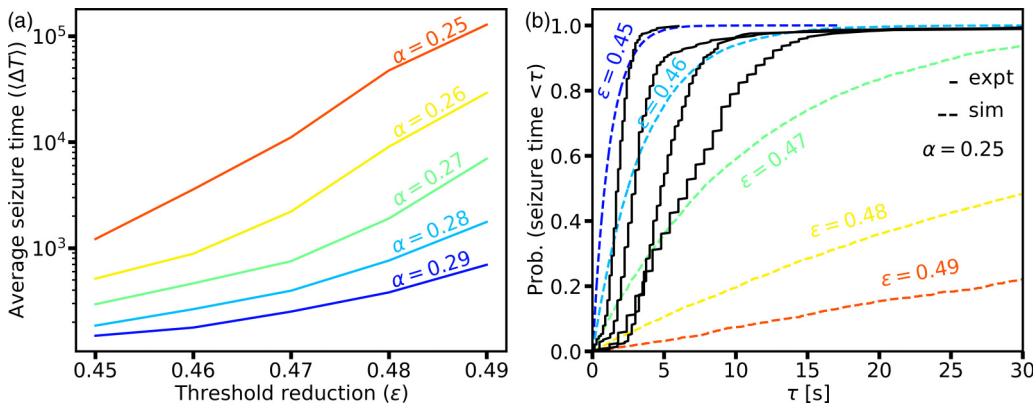

FIG. 3. Switching times in model simulations and experiments. (a) Average seizure time as a function of threshold reduction ϵ, for varying values of inhibition α. The error bars show a 95% confidence interval, here being hardly visible because they are so small. (b) Probability of seizure times being larger than τ shown for varying values of threshold reduction and fixed inhibition $\alpha = 0.25$. Four different exemplary spiking data sets are shown as black lines.
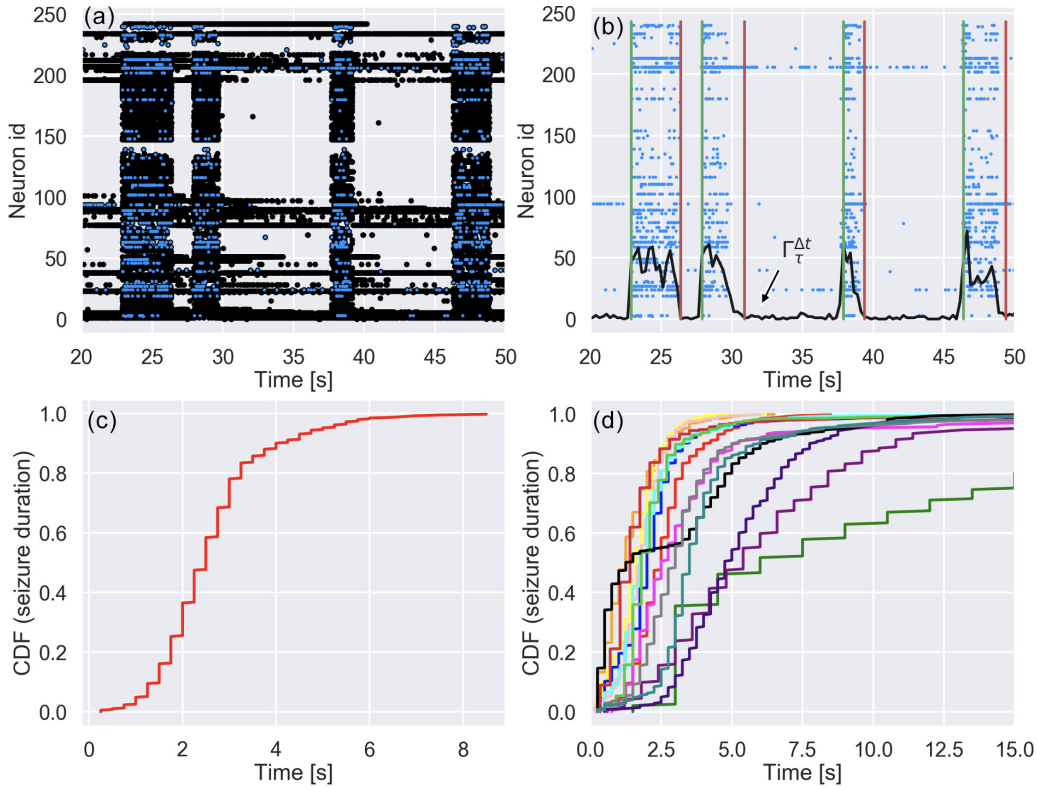
FIG. 4. Extracting seizure times from data. (a) A raster plot is shown for a representative piece of spiking data. A black circular marker is placed at every time (x axis) for the corresponding neuron (y axis). Blue dots are plotted to represent those spikes that were kept after the subsampling. (b) Only the blue dots from (a) are shown, with a black line representing the averaged spiking rate, $\Gamma_\tau^{\Delta t}$. Green and red vertical lines mark the beginning and end of an avalanche, respectively. (c) The extracted cumulative distribution function of seizure durations for an exemplary data set is shown with a red line. (d) The same thing as (c), but with all 15 data sets plotted in varying colors.

neuron systems has found this characteristic-earthquake distribution [9,19,27,41], and the runaway avalanches in our model compare closely to dragon king avalanches [27] as well as giant depolarizing events [42,43].

However, the exciting result of our work is that a simple model with weakening can not only produce this "characteristic distribution," but also gives predictions for the average time spent in a seizure state (or "up-state" [19]). Importantly, this means that studying these switching times (rather than avalanche properties directly) is not vulnerable to the problem of subsampling in neuron data sets [26]. This means that a subsampled data set will give the same results for switching times as the fully sampled set (since we see roughly the same burst outline even *after* subsampling; see Appendix A).

We compared the statistics of burst times in the experimental (*in vitro*) data [30] (e.g., time spent in the high or low activity states) to see if the trends resemble the predictions of our model. Our simple model has only a few limited ingredients, but we are still able to capture several features of the data. In particular, we compare the high activity state in experiments to our model's seizure state. We find that the average time spent in the high activity state roughly follows a Poissonian distribution, consistent with the prediction of our model for the seizure state [22]see Fig. 3(b) and Appendix A. Further, comparing four separate data sets (i.e., from different brain slices on different chips), we find a possible explanation for differing burst statistics: that the effective memory from

sample to sample is differing, as exemplified by Fig. 3(b). We would also point out that the discrepancy between model and data, particularly for small τ, is likely attributed to the algorithm's poor ability to find small seizures—due to its threshold nature and preprocessing (see Appendix A).

The switching phenomenon also provides a possible mechanism that is responsible for excessive brain activity [27,42–44]. This is because the seizure state nucleates out of the normal state at random—that just means that if the avalanche size surpasses a critical value, it turns into a runaway avalanche, transitioning the network into the seizure state. This random occurrence might explain why it is difficult to find reliable precursors to seizures. The nucleation of a seizure state is ultimately a consequence of the dynamic threshold weakening. The nucleation size, i.e., the critical avalanche size needed to trigger this switching, $S_{cr} \sim (1 - \epsilon)N/(1 - \alpha)$, depends on N, α, and ϵ. By measuring this size, it may be possible to estimate where a real system lies in $\{\alpha, \epsilon\}$ space. More importantly, by changing the various parameters through appropriate drugs, it may be possible to increase the nucleation size so that seizure episodes are less likely and thus greatly suppressed.

Our work also encourages a discussion about which critical point is controlling the system. Inhibition-induced desynchronization is seen in experiments [42,45,46] and indeed many models suggest that a synchronization transition is controlling the system [17,44,47–51]. On the other hand, several

```
Flag=0
τ = [0, Δt, 2Δt, ... , 3600]
For i in τ:
        If (Flag==1) & (Γ_τ^Δt < T_end):
                burst_end_time=i
                Flag=0
        elif (Flag==0) & (Γ_τ^Δt > T_start):
                burst_start_time=i
                Flag=1
```

FIG. 5. Pseudocode describing an algorithm for identifying burst start and stop times. A flag is set to zero initially, and switches between zero and one to capture the moments when $\Gamma_\tau^{\Delta t}$ moves above and below a threshold, marking the start and end of a burst, respectively.

other models suggest that the critical point is that of directed percolation, describing the transition between the active and absorbing states [6–11]. Even combinations of the two have been suggested [10,17,52]. We are instead suggesting a close cousin to directed percolation, the weakened-depinning transition, which resembles the problem of an elastic interface moving in a disordered environment [53] with dynamic threshold weakening [23]. In analogy, cells of the interface correspond to neurons, their slipping corresponds to neurons spiking, the elastic interactions correspond to the synaptic connections between neurons, and the disorder in slipping thresholds across the interface corresponds to the heterogeneity of spike thresholds among many neurons. The feature that is not directly reflected in the neural system is the dynamic weakening, which is the key ingredient out of which the quasiperiodic runaway events emerge, whose connections to oscillations in neuronal systems warrant further investigation.

Further, the question of self-organized criticality (SOC) that arises in much of the neuroscience literature [1,5,7,14,16,19,28,29] can be studied in the context of domain wall motion in magnets, where global dipolar effects called "demagnetization fields" can self-organize the wall to the center of the system [29,54,55]. These demagnetization fields are equivalent to inhibition in our system, and an important prediction of [29] is that SOC is only realized with infinite-ranged (global) weak demagnetization fields. This would suggest that real neuronal systems (i.e., those with an underlying network structure) are not expected to be self-organized critical, but rather near an ordinary critical

point, and that they can be tuned closer to or farther away from criticality by tuning parameters such as inhibition strength and weakening. Future directions include extending this work beyond mean-field theory models to include, e.g., these underlying network structures.

Lastly, we wish to mention that similar recurrent large avalanches can be obtained by overshoots that may be caused, for example, by temporary increases in the coupling between neurons [23]. Here we use the weakening as a representative of a class of many different mechanisms that can cause such large avalanches. The results discussed here should apply in similar ways to other mechanisms, such as overshoots or temporary coupling increases. In either case, the large recurrent avalanches may be similar to seizures, so it is of great interest to understand their statistics.

V. CONCLUSION

In this paper, we investigated a simple model for spiking neurons and showed how the addition of a different feature—dynamical weakening—produces qualitatively similar behavior to seizures. Specifically, our results predict a regular (normal) and epileptic (seizure) state, and the possibility of switching from one to the other in any finite-size system. We found a prediction for seizure duration statistics that does not require the definition of an avalanche, allowing us to compare with empirical data. This prediction may not only help connect past conflicting research on neuronal avalanches, but also suggests a different perspective of seizures from the point of view of material fracture. The work also informs the debate on which critical point is controlling neuronal avalanches; namely, the weakened depinning universality class, with *tuned* rather than *self-organized* criticality.

APPENDIX A: EXTRACTING SEIZURE STATE LIFETIMES FROM EXPERIMENTAL DATA

We used the data sets openly provided in [30] to make empirical observations of the switching time distributions. The raw data ($n = 15$, mouse cortical slices above 512 electrode array) consist of labeled spike times [i.e., the seventh neuron fired at time $t = 400 \rightarrow (7, 400)$]. We could visualize this, for instance, as a "raster plot" [see Fig. 4(a)], where a single dot is shown for each labeled spike-time-tuple in the data set, located at $x =$ spike time (e.g., 400) and $y =$ neuron ID (e.g.,

Data set	1	2	3	4	5	6	7	8	9	10	11	12	13	14	15
SpikeMax (No. x 1E3)	2.5	5	2.5	5	5	4	4	10	4	5	5	5	8	3	5
Δt (s)	0.25	0.25	0.2	0.15	0.25	0.6	0.15	0.25	0.35	0.25	0.25	0.25	0.25	0.25	0.25
T_{start} (No.)	20	20	10	20	10	50	55	50	40	30	100	50	15	40	40
T_{end} (No.)	3	15	3	3	3	10	2	6	6	24	3	3	3	3	3

FIG. 6. Parameters chosen for the algorithm. For each of the 15 studied data sets, the parameters are used for both the subsampling algorithm (SpikeMax) and the burst finding algorithm (Δt, T_{start} and T_{end}).
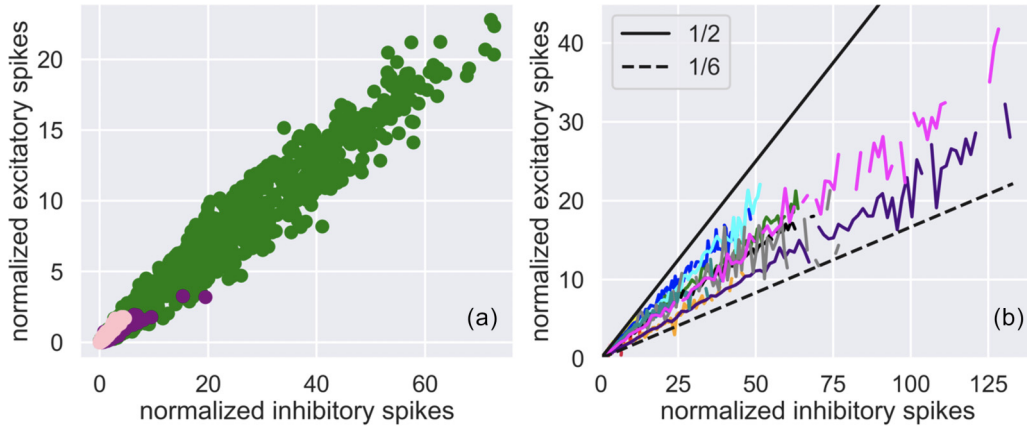
FIG. 7. Inhibitory neurons spike roughly proportional to excitatory neurons on average. (a) Each dot represents an avalanche, with the *y* value representing the number of excitatory spikes in the avalanche, normalized by the total number of excitatory species in the sample. Similarly, the *x* value represents the number of inhibitory spikes, again normalized by the number of inhibitory species in the sample. Three example data sets are shown in green, magenta, and light pink. (b) The scatter plot from (a) is represented by a bin-averaged line, shown in different colors for the 15 different samples studied in this work. The solid and dashed lines show the bound of the linear slope of the data, lying between 1/2 and 1/6, respectively.

7). In doing so, we observe (in all data sets) synchronous activity where almost all the neurons in the system are spiking. These regions of activity are usually referred to as "up-states" and the regions of relative inactivity between them are referred to as "down-states." We will be interested in characterizing how long the system dwells in this up-state (i.e., "seizure times").

To this end, we extract the start and end times of each labeled up-state in the 1-hour-long recording. Using a method derived from [56], we will first remove tonically spiking neurons (i.e., neurons that never seem to stop spiking, no matter what state the rest of the system is in). We perform this by simply removing neurons that spike more than a prescribed number of times ("SpikeMax") in the 1-hour-long recording. We note that this simply makes our algorithm more robust while not obstructing the true start vs end times of an up-state (if we do not remove too many neurons). This is because the synchronous activity we seek to characterize is relatively insensitive to the subsampling; by this we just mean that the synchronous up-state is a global feature of the system that is still very apparent even after subsampling [see Fig. 4(b)].

With this preprocessing of the data complete, we can cook up quite a robust algorithm for identifying the start and end times of the up-states. Starting from the set of tuples, we can construct a global list of spike times t_i (e.g., ignoring neuron labels for now) and order it $t_i \rightarrow \{t_i | \forall i, j > i, t_i < t_j\}$. The next step is to coarse grain this list (in time with bin width Δt) such that we construct the sequence representing the inverse of the global spiking rate, $r_{\tau,\Delta t}^{-1} \equiv \Gamma_\tau^{\Delta t} = \sum_{i=\tau}^{i=\tau+\Delta t} \delta_{i,t_i}$ [Fig. 4(b), black line]. We can use a simple

algorithm (outlined in pseudocode in Fig. 5) that picks out a start time [Fig. 4(b), vertical green lines] wherever the signal rises above some threshold, $\Gamma_\tau^{\Delta t} > T_{\text{start}}$, and, equivalently, picks out the end time [Fig. 4(b), vertical red lines] when the signal subsequently crosses below a (separate) threshold, $\Gamma_\tau^{\Delta t} < T_{\text{end}}$.

We point out that the algorithm is not perfect, for instance, in the second up-state of Fig. 4(b), we see that the end time is overestimated. This means the threshold T_{end} was not perfect. The parameters SpikeMax, Δt, T_{start}, and T_{end} are chosen to get the most accurate estimation of start and end times. We catalog the chosen parameters for each data set in Fig. 6.

APPENDIX B: INHIBITORY NEURONS SPIKE PROPORTIONALLY TO EXCITATORY ONES.

In this Appendix, we briefly discuss the validity of an assumption made in the manuscript—that the averaged spiking rate of the inhibitory neurons is, at most, a constant away from that of the excitatory spiking rate. With recently discerned information about species labels in the data studied above, we are at will to compare the number of excitatory spikes in an avalanche to the number of inhibitory spikes in an avalanche [Fig. 7(a), three data sets used in main paper]. Since there is a different number of excitatory than inhibitory neurons, we normalize the spike count in each avalanche by the number of excitatory neurons and inhibitory neurons in the system, respectively. We see a striking trend towards linearity and further confirm this with a bin average over the *x* axis, for all $n = 15$ data sets [Fig. 7(b)], where the slopes range between 1/2 and 1/6.

[1] J. M. Beggs and D. Plenz, Neuronal avalanches in neocortical circuits, J. Neurosci. **23**, 11167 (2003).

[2] A. J. Fontenele, N. A. De Vasconcelos, T. Feliciano, L. A. Aguiar, C. Soares-Cunha, B. Coimbra, L. Dalla Porta, S. Ribeiro, A. J. Rodrigues, N. Sousa, P. V. Carelli, and M. Copelli, Criticality between cortical states, Phys. Rev. Lett. **122**, 208101 (2019).

[3] T. Petermann, T. C. Thiagarajan, M. A. Lebedev, M. A. L. Nicolelis, D. R. Chialvo, and D. Plenz, Spontaneous cortical activity in awake monkeys composed of neuronal avalanches, Proc. Natl. Acad. Sci. **106**, 15921 (2009).

[4] N. Friedman, S. Ito, B. A. Brinkman, M. Shimono, R. E. Deville, K. A. Dahmen, J. M. Beggs, and T. C. Butler, Universal critical dynamics in high resolution neuronal avalanche data, Phys. Rev. Lett. **108**, 208102 (2012).

[5] V. Pasquale, P. Massobrio, L. L. Bologna, M. Chiappalone, and S. Martinoia, Self-organization and neuronal avalanches in networks of dissociated cortical neurons, Neuroscience **153**, 1354 (2008).

[6] M. A. Buice and J. D. Cowan, Field-theoretic approach to fluctuation effects in neural networks, Phys. Rev. E **75**, 051919 (2007).

[7] L. Brochini, A. De Andrade Costa, M. Abadi, A. C. Roque, J. Stolfi, and O. Kinouchi, Phase transitions and self-organized criticality in networks of stochastic spiking neurons, Sci. Rep. **6**, 35831 (2016).

[8] M. Girardi-Schappo, L. Brochini, A. A. Costa, T. T. Carvalho, and O. Kinouchi, Synaptic balance due to homeostatically self-organized quasicritical dynamics, Phys. Rev. Res. **2**, 012042(R) (2020).

[9] A. Costa, L. Brochini, and O. Kinouchi, Self-organized supercriticality and oscillations in networks of stochastic spiking neurons, Entropy **19**, 399 (2017).

[10] Y. Karimipanah, Z. Ma, and R. Wessel, Criticality predicts maximum irregularity in recurrent networks of excitatory nodes, PLoS ONE **12**, e0182501 (2017).

[11] L. D. Porta and M. Copelli, Modeling neuronal avalanches and long-range temporal correlations at the emergence of collective oscillations: Continuously varying exponents mimic M/EEG results, PLoS Comput. Biol. **15**, e1006924 (2019).

[12] W. L. Shew, H. Yang, T. Petermann, R. Roy, and D. Plenz, Neuronal avalanches imply maximum dynamic range in cortical networks at criticality, J. Neurosci. **29**, 15595 (2009).

[13] W. L. Shew, H. Yang, S. Yu, R. Roy, and D. Plenz, Information capacity and transmission are maximized in balanced cortical networks with neuronal avalanches, J. Neurosci. **31**, 55 (2011).

[14] M. Rubinov, O. Sporns, J.-P. Thivierge, and M. Breakspear, Neurobiologically realistic determinants of self-organized criticality in networks of spiking neurons, PLoS Comput. Biol. **7**, e1002038 (2011).

[15] A. Das and A. Levina, Critical neuronal models with relaxed timescale separation, Phys. Rev. X **9**, 021062 (2019).

[16] J. N. Teramae and T. Fukai, Local cortical circuit model inferred from power-law distributed neuronal avalanches, J. Comput. Neurosci. **22**, 301 (2007).

[17] S. di Santo, P. Villegas, R. Burioni, and M. A. Muñoz, Landau-Ginzburg theory of cortex dynamics: Scale-free avalanches emerge at the edge of synchronization, Proc. Natl. Acad. Sci. **115**, E1356 (2018).

[18] Z. Lu, S. Squires, E. Ott, and M. Girvan, Inhibitory neurons promote robust critical firing dynamics in networks of integrate-and-fire neurons, Phys. Rev. E **94**, 062309 (2016).

[19] F. Lombardi, H. J. Herrmann, C. Perrone-Capano, D. Plenz, and L. de Arcangelis, Balance between excitation and inhibition controls the temporal organization of neuronal avalanches, Phys. Rev. Lett. **108**, 228703 (2012).

[20] M. Yaghoubi, T. de Graaf, J. G. Orlandi, F. Girotto, M. A. Colicos, and J. Davidsen, Neuronal avalanche dynamics indicates different universality classes in neuronal cultures, Sci. Rep. **8**, 3417 (2018).

[21] J. S. Coombs, J. C. Eccles, and P. Fatt, The specific ionic conductances and the ionic movements across the motoneuronal membrane that produce the inhibitory post-synaptic potential, J. Physiol. **130**, 326 (1955).

[22] K. Dahmen, D. Ertaş, and Y. Ben-Zion, Gutenberg-Richter and characteristic earthquake behavior in simple mean-field models of heterogeneous faults, Phys. Rev. E **58**, 1494 (1998).

[23] D. S. Fisher, K. Dahmen, S. Ramanathan, and Y. Ben-Zion, Statistics of earthquakes in simple models of heterogeneous faults, Phys. Rev. Lett. **78**, 4885 (1997).

[24] T. Salners, K. E. Avila, B. Nicholson, C. R. Myers, J. Beggs, and K. A. Dahmen, Recurrent activity in neuronal avalanches, Sci. Rep. **13**, 4871 (2023).

[25] K. A. Dahmen, Y. Ben-Zion, and J. T. Uhl, Micromechanical model for deformation in solids with universal predictions for stress-strain curves and slip avalanches, Phys. Rev. Lett. **102**, 175501 (2009).

[26] J. P. Neto, F. P. Spitzner, and V. Priesemann, Sampling effects and measurement overlap can bias the inference of neuronal avalanches, PLoS Comput. Biol. **18**, e1010678 (2022).

[27] L. de Arcangelis, Are dragon-king neuronal avalanches dungeons for self-organized brain activity? Eur. Phys. J.: Spec. Top. **205**, 243 (2012).

[28] M. G. Kitzbichler, M. L. Smith, S. R. Christensen, and E. Bullmore, Broadband criticality of human brain network synchronization, PLOS Comput. Biol. **5**, e1000314 (2009).

[29] O. Narayan, Self-similar Barkhausen noise in magnetic domain wall motion, Phys. Rev. Lett. **77**, 3855 (1996).

[30] S. Ito, F.-C. Yeh, N. M. Timme, P. Hottowy, A. M. Litke, and J. M. Beggs, Spontaneous spiking activity of hundreds of neurons in mouse somatosensory cortex slice cultures recorded using a dense 512 electrode array, https://www.jneurosci.org/content/16/14/4438 (unpublished).

[31] J. P. Hobbs, J. L. Smith, and J. M. Beggs, Aberrant neuronal avalanches in cortical tissue removed from juvenile epilepsy patients, J. Clin. Neurophysiol. **27**, 380 (2010).

[32] D. Hsu, W. Chen, M. Hsu, and J. M. Beggs, An open hypothesis: Is epilepsy learned, and can it be unlearned? Epilepsy Behav. **13**, 511 (2008).

[33] C. Meisel, A. Storch, S. Hallmeyer-Elgner, E. Bullmore, and T. Gross, Failure of adaptive self-organized criticality during epileptic seizure attacks, PLoS Comput. Biol. **8**, e1002312 (2012).

[34] X. Li, J. Polygiannakis, P. Kapiris, A. Peratzakis, K. Eftaxias, and X. Yao, Fractal spectral analysis of pre-epileptic seizures in terms of criticality, J. Neural Eng. **2**, 11 (2005).

[35] C. Meisel and T. Loddenkemper, Seizure prediction and intervention, Neuropharmacology **172**, 107898 (2020).

[36] S. Auno, L. Lauronen, J. Wilenius, M. Peltola, S. Vanhatalo, and J. M. Palva, Detrended fluctuation analysis in the presurgical evaluation of parietal lobe epilepsy patients, Clinic. Neurophysiol. **132**, 1515 (2021).

[37] M. I. Maturana, C. Meisel, K. Dell, P. J. Karoly, W. D'Souza, D. B. Grayden, A. N. Burkitt, P. Jiruska, J. Kudlacek, J. Hlinka, M. J. Cook, L. Kuhlmann, and D. R. Freestone, Critical slowing

down as a biomarker for seizure susceptibility, Nat. Commun. **11**, 2172 (2020).

[38] O. Arviv, M. Medvedovsky, L. Sheintuch, A. Goldstein, and O. Shriki, Deviations from critical dynamics in interictal epileptiform activity, J. Neurosci. **36**, 12276 (2016).

[39] D. Burrows, G. Diana, B. Pimpel, F. Moeller, M. Richardson, D. Bassett, M. Meyer, and R. Rosch, Single-cell networks reorganise to facilitate whole-brain supercritical dynamics during epileptic seizures, bioRxiv:2021.10.14.464473.

[40] V. Zimmern, Why brain criticality is clinically relevant: A scoping review, Front. Neural Circ. **14**, 54 (2020).

[41] I. Osorio, M. G. Frei, D. Sornette, J. Milton, and Y. C. Lai, Epileptic seizures: Quakes of the brain? Phys. Rev. E **82**, 021919 (2010).

[42] Y. Ben-Ari, E. Cherubini, R. Corradetti, and J. L. Gaiarsa, Giant synaptic potentials in immature rat CA3 hippocampal neurones, J. Physiol. **416**, 303 (1989).

[43] L. M. de la Prida and J. V. Sanchez-Andres, Heterogeneous populations of cells mediate spontaneous synchronous bursting in the developing hippocampus through a frequency-dependent mechanism, Neuroscience **97**, 227 (2000).

[44] L. M. de la Prida, S. Bolea, and J. V. Sanchez-Andres, Analytical characterization of spontaneous activity evolution during hippocampal development in the rabbit, Neurosci. Lett. **218**, 185 (1996).

[45] J. P. Wuarin and F. E. Dudek, Electrographic seizures and new recurrent excitatory circuits in the dentate gyrus of hippocampal slices from kainate-treated epileptic rats, J. Neurosci. **16**, 4438 (1996).

[46] O. Garaschuk, E. Hanse, and A. Konnerth, Developmental profile and synaptic origin of early network oscillations in the

CA1 region of rat neonatal hippocampus, J. Physiol. **507**, 219 (1998).

[47] B. Percha, R. Dzakpasu, M. Zochowski, and J. Parent, Transition from local to global phase synchrony in small world neural network and its possible implications for epilepsy, Phys. Rev. E **72**, 031909 (2005).

[48] J. Lehnert, T. Dahms, P. Hövel, and E. Schöll, Loss of synchronization in complex neuronal networks with delay, Europhys. Lett. **96**, 60013 (2011).

[49] S. R. Campbell, D. L. L. Wang, and C. Jayaprakash, Synchrony and desynchrony in integrate-and-fire oscillators, Neural Comput. **11**, 1595 (1999).

[50] M. G. Rosenblum and A. S. Pikovsky, Controlling synchronization in an ensemble of globally coupled oscillators, Phys. Rev. Lett. **92**, 114102 (2004).

[51] Y. Shen, Z. Hou, and H. Xin, Transition to burst synchronization in coupled neuron networks, Phys. Rev. E **77**, 031920 (2008).

[52] S.-S. Poil, R. Hardstone, H. D. Mansvelder, and K. Linkenkaer-Hansen, Critical-state dynamics of avalanches and oscillations jointly emerge from balanced excitation/inhibition in neuronal networks, J. Neurosci. **32**, 9817 (2012).

[53] D. S. Fisher, Collective transport in random media: From superconductors to earthquakes, Phys. Rep. **301**, 113 (1998).

[54] J. S. Urbach, R. C. Madison, and J. T. Markert, Interface depinning, self-organized criticality, and the Barkhausen effect, Phys. Rev. Lett. **75**, 276 (1995).

[55] G. Durin and S. Zapperi, Scaling exponents for Barkhausen avalanches in polycrystalline and amorphous ferromagnets, Phys. Rev. Lett. **84**, 4705 (2000).

[56] D. Bakkum, M. Radivojevic, U. Frey, F. Franke, A. Hierlemann, and H. Takahashi, Parameters for burst detection, Front. Comput. Neurosci. **7**, 1 (2014).